



Oxygen stabilized W–Ag films for environmental antibacterial applications

Tao FU¹, Li-jun WANG¹, Ying-jie WANG¹, Dong-zhen CHEN², Po-wan SHUM³

1. Key Laboratory of Biomedical Information Engineering of Ministry of Education, School of Life Science and Technology, Xi'an Jiaotong University, Xi'an 710049, China;
2. School of Materials Science and Engineering, Xi'an Polytechnic University, Xi'an 710048, China;
3. Asahi Group Co. Ltd., Kwun Tong, Hong Kong, China

Received 29 October 2021; accepted 1 March 2022

Abstract: Oxygen was added into sputter deposited tungsten films to reduce residual stress of the films, and silver with content up to 14.3 at.% was further added for antibacterial functionalization. The films were analyzed by SEM-EDX, XPS and XRD. Only X-ray diffraction peaks from β -W or W_3O phase were detected for the films. Oxygen and silver existed mainly as solid solution atoms in the films. Silver addition decreased hardness (still ≥ 10.3 GPa) and elastic modulus of the films. The potentiodynamic polarization demonstrated lower corrosion current density of the WO film than that of the tungsten film, and silver changed corrosion behavior of the films. The Ag-depleted tungsten oxide layer on the film surface suppressed the release of silver ions in water. The WOAg films had good antibacterial activity with *E.coli* bacteria. The WOAg films would be useful in environmental and other antimicrobial applications.

Key words: tungsten film; tungsten oxide; silver segregation; residual stress; antibacterial coating

1 Introduction

Bacteria and virus related infections pose a great threat to the people worldwide [1,2]. Pathogenic bacteria and virus spread through breathing, speaking, coughing, sneezing, and sweat contact, etc., in clinical, public, family and other environments [3–5]. It is of crucial significance to stop the spread of pathogenic microbes by efficient measures including antimicrobial agents. The inorganic antibacterial agents, e.g. metallic ions type and photocatalytic type [6–9], have the advantages of good structural stability, high antimicrobial efficiency and enough bio-safety. Among the metallic elements exhibiting bactericidal property (Ag, Cu, Zn, W, etc [6,7,9,10]), silver is a well-known and effective antimicrobial with a wide spectrum against many kinds of

drug-resistant bacteria, even virus [1] and good cytocompatibility [11–13].

Vapor deposited nitride and diamond-like carbon films are known to possess high hardness, good chemical stability and wear resistance, and therefore silver is added into these ceramic coatings for antibacterial applications. For example, TiN–Ag [14], TaN–Ag [15] and DLC–Ag [16,17] films prepared by magnetron sputtering exhibited high mechanical properties and good antibacterial property. However, silver segregation often occurs for the ceramic–silver coatings [14–17] due to different natures of the film matrix and silver. The segregation of silver nanoparticles would enhance antibacterial property, but raise the biosafety concern of silver. Therefore, silver-containing transition metal antibacterial films are developed, e.g. Ti–Ag films [18,19], Nb–Ag film [18] and W–Ag films [20].

Corresponding author: Tao FU, Tel: +86-29-82669021, E-mail: taofu@xjtu.edu.cn;

Dong-zhen CHEN, Tel: +86-29-82330170, E-mail: chendz365@xpu.edu.cn

DOI: 10.1016/S1003-6326(22)66125-9

1003-6326/© 2023 The Nonferrous Metals Society of China. Published by Elsevier Ltd & Science Press

It is known that tungsten is a hard, anti-bacterial [10] and well biocompatible metal [21,22]. Our previous study showed that W–Ag films had high hardness and good antibacterial activity, but adhesion of W film was affected by the compressive residual stress [20]. It was reported that the addition of oxygen released compressive residual stress of the WO films [23]. In this work, oxygen was added into the sputter prepared W–Ag films with silver content up to 14.3 at.% in order to avoid the negative effect of residual stress. Microstructure, film hardness, anticorrosion behavior and antibacterial property of the coating samples were systematically studied for the potential environmental and other antimicrobial applications.

2 Experimental

2.1 Sample preparation

The WOAg films were prepared on slide glass, silicon wafers and stainless steel plates (316L, 10 mm × 10 mm × 1.0 mm) by a reactive magnetron sputtering system (UDP–650, Teer Coatings Ltd., Fig. 1). The substrates were cleaned by degreasing

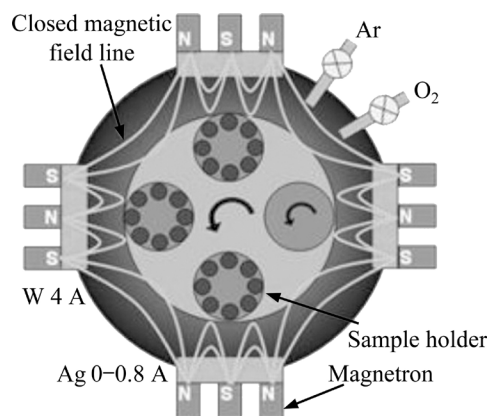


Fig. 1 Schematic drawing of UDP coating system (Teer Coatings Ltd.)

and ultrasonic cleaning. In the deposition system one W and one Ag targets (purity >99.9%) were fixed for film preparation. After plasma cleaning using pure Ar gas, the films were deposited with Ar flow rate 30 mL/min, oxygen flow rate 30 mL/min, tungsten target current 4.0 A, silver target current 0–0.8 A, substrate bias –50 V and deposition time 110 min. The substrate holder was rotated at 10 r/min during plasma cleaning and film deposition. The WOAg film samples were noted as AX and AX-Y, in which X meant silver target current and Y was the silver content (Table 1). Tungsten film (noted as O00) and WAg film with 4.2 at.% silver were also prepared for comparison.

2.2 Material characterization and antibacterial test

Film thickness and surface roughness of the samples were measured with a surface profilometer. Surface of the film samples was analyzed with scanning electron microscopy (SEM, FEI Quanta 600F) equipped with energy-dispersive X-ray analysis (EDX) and X-ray photoelectron spectroscopy (XPS, VG K-Alpha, Al K_{α}). Crystallographic structure of the coating samples was analyzed by X-ray diffraction (XRD, X'Pert PRO, Cu K_{α}). Mechanical properties of the coatings were measured by a Nano Indenter, G200. Anticorrosion behavior of the stainless steel group samples was assessed with an electrochemical workstation. The coated glass samples with the size of 12.5 mm × 12.5 mm were immersed in 10 mL deionized water at room temperature (25 °C) for different time, and the ion concentrations were measured by the inductively coupled plasma mass spectrometry (ICP-MS, NexIon 350D, PE).

Antibacterial property of the samples was assessed by the agar plate counting method against *E. coli*, which are typical Gram negative bacteria

Table 1 Deposition parameters, thickness (T), deposition rate (R), chemical composition and surface roughness (R_a) of WOAg films on Si(111) substrate

Sample	O ₂ flow rate/ (mL·min ⁻¹)	$I(\text{Ag})$ / A	T / μm	R / (nm·min ⁻¹)	W content/ at. %	O content/ at. %	Ag content/ at. %	R_a / nm
O00	0	0	0.86	7.8	91.7	8.3	0	1.0
A00	30	0	1.80	16.4	40.9	59.1	0	1.2
A02	30	0.2	1.92	17.4	38.0	60.3	1.7	1.0
A04	30	0.4	2.54	23.1	34.7	59.8	5.5	1.0
A06	30	0.6	2.59	23.6	31.1	59.5	9.4	1.2
A08	30	0.8	2.95	26.8	27.2	58.5	14.3	2.2

encountered in environmental, food and biomedical applications. The detailed experimental process was described in Ref. [20]. The samples were tested at least twice independently.

3 Results and discussion

3.1 SEM-EDX, film thickness, roughness, XRD and XPS analyses

The WO and WOAg films on glass, silicon and steel substrates are adherent and smooth. The SEM surface images in Fig. 2 show that, the surface of Sample A00 is rather smooth, nanoparticles are observed for Samples A02–A08, and the number of particles increases with Ag target current. In the backscattered electron image (Fig. 2(e)), the lower gray level of the nanoparticles indicates that they consist of mainly silver. The nanoparticles grow larger due to Ostwald ripening after ageing for 2.5 years. The areal EDX analysis indicates that silver content of the films increases with the silver target current, e.g. being 5.5 and 14.3 at.% for A04 and A08 (Table 1). The oxygen content is nearly constant, being around 60 at.%. The film thickness measured by the surface profilometer ranges from 0.86 to 2.95 μm , and the deposition rate increases with oxygen flow rate and silver target current. However, the surface roughness of the films is kept as low as 1.0–2.2 nm (Table 1).

For the films deposited on silicon substrate, the diffraction peaks at $2\theta=35.5^\circ$, 39.9° and 43.9° can be ascribed to (200), (210) and (211) peaks, respectively of cubic W (β -W, ICDD file #47-1319) or W_3O phase (ICDD file #41-1230 [24], Fig. 3). The silver peaks are not detected for Samples A02–A06, but a broad hump centered at $2\theta=38.1^\circ$ appears for Sample A08, which is ascribed to Ag(111) plane.

The cubic crystal structure of the W film (Sample O00) is not changed even when oxygen flow is increased to 30 mL/min (Sample A00). Oxygen atoms thus exist in W lattice as interstitial atoms due to their small size (radius 66 pm) compared with that of W atoms (radius 130 pm). It was suggested that β -W is a metastable phase with the interstitial oxygen as stabilizer [25]. It was reported that the addition of oxygen above 30 at.% nearly released the compressive residual stress of the WO films [23]. Tungsten and silver are immiscible due to the large positive enthalpy in mixing [26], but W has similar atomic radius to that of Ag (134 pm). It is postulated that silver mainly forms the meta-stable solid solution with WO films under the energetic ion bombardment during film growth.

Surface composition of Samples A00–A08 was examined by XPS analysis, with the spectra of Sample A06 shown in Fig. 4. Strong W 4f double

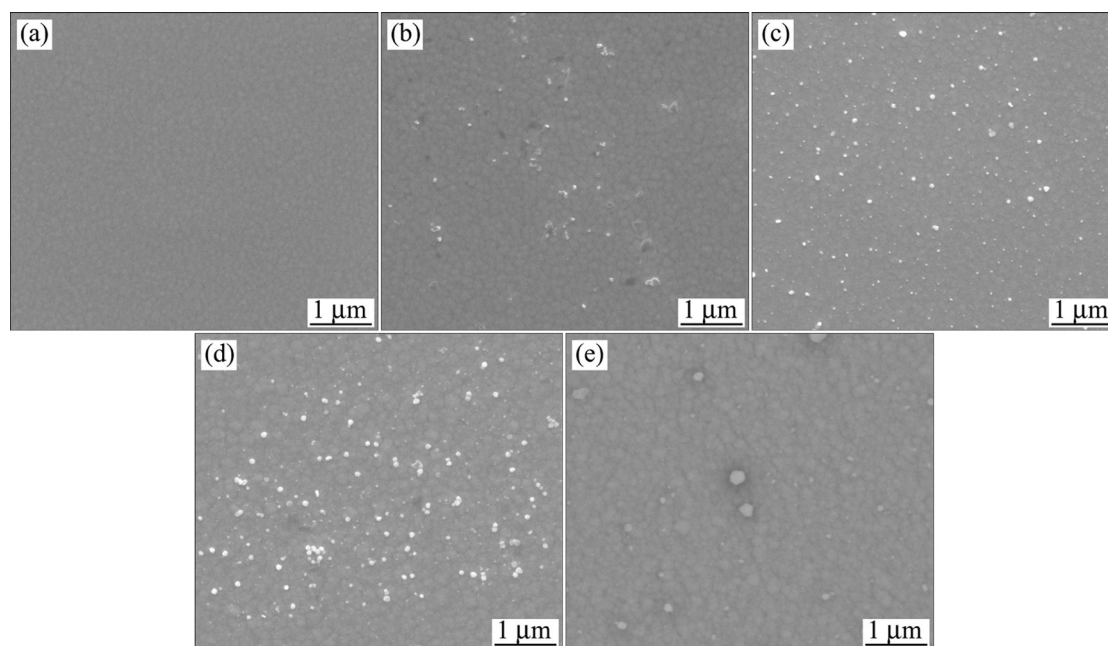


Fig. 2 Surface secondary electron images of WOAg films on silicon substrate: (a) A00; (b) A02; (c) A06; (d) A08; (e) Backscattered electron image of Sample A08 after ageing for 2.5 years

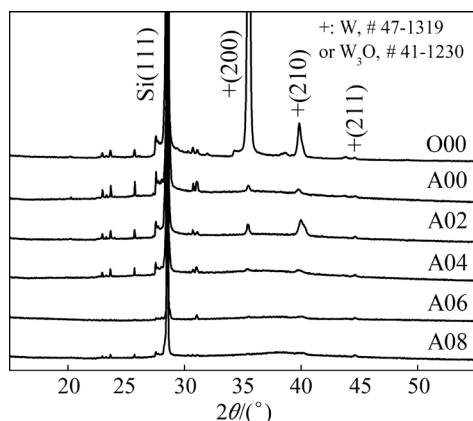


Fig. 3 XRD patterns of W, WO and WOAg film samples with silicon substrate

peaks at 37.9 eV ($4f_{5/2}$) and 35.8 eV ($4f_{7/2}$) are indicative of tungsten oxide (WO_3) on the surface of the film. The small peak at 33.6 eV is likely related to metallic tungsten ($4f_{5/2}$ peak, corresponding to $4f_{7/2}$ peak at 31.5 eV). The widening of the peaks after 30 s sputter etching reveals the sub-oxidation states of tungsten below the top surface layer. In O 1s spectra, the main peak at 530.7 eV is attributed to oxygen atoms in W–O lattice, and the shoulder peak at 532.3 eV may come from the surface-adsorbed oxygen species such as O^- [26,27] during the stay in air before XPS test. In Ag 3d spectra, the double peaks are located at 374.1 eV ($3d_{3/2}$) and 368.1 eV ($3d_{5/2}$). Thus, silver exists mainly in metallic state in the film.

The elemental ratios of the films measured by EDX and XPS are comparatively shown in Fig. 4. The O/W atomic ratio of Samples A00–A08 obtained by XPS (2.6–3.2) is much higher than that of Sample A00 obtained by EDX (being 1.4). This reveals further oxidation of tungsten and enrichment of oxygen on top surface of the WOAg films during ageing in air, like the case of W film (Fig. 5(a)). As for the Ag/W atomic ratio, the values obtained by XPS are much lower than those obtained by EDX for Samples A04–A08. This indicates depletion of silver on top surface of these films. In comparison, the WAg film with 4.2 at.% Ag measured by EDX has the similar Ag/W ratio obtained by XPS (Fig. 5(b)). Thus, serious silver segregation for the ceramic-silver coatings [14–16] does not occur for the present WOAg and WAg films. The even vertical distribution of silver in the films would ensure sustainable release of silver ions and reliable biological properties of the films.

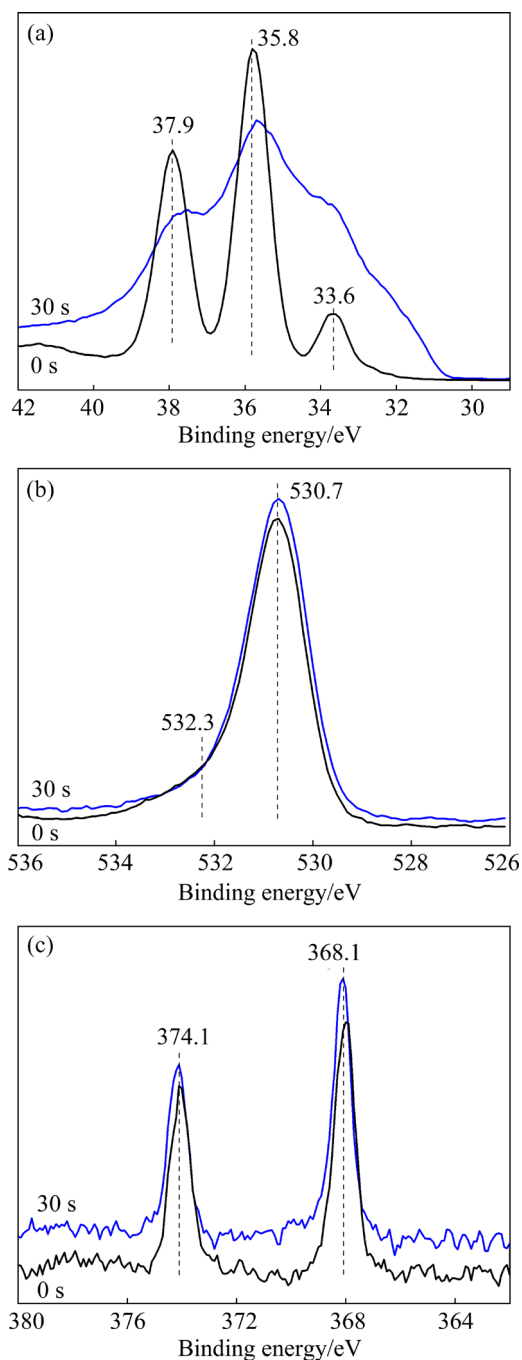


Fig. 4 XPS high-resolution W 4f (a), O 1s (b) and Ag 3d (c) spectra of Sample A06 with silicon substrate before and after 30 s sputter etching

3.2 Nanohardness and corrosion tests

Hardness of the films was measured by nanoindentation. The load–displacement curves of the film samples are shown in Figs. 6(a–c). It can be seen that the curves coincide with each other for Samples A00–A08, but the curves are not overlapped for O00. Sputter deposited tungsten film has high compressive residual stress, the grown

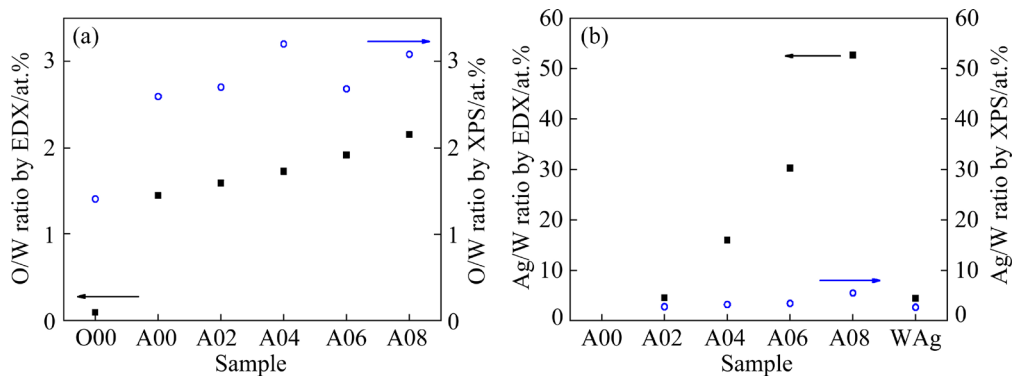


Fig. 5 O/W (a) and Ag/W (b) atomic ratios of W, WO, WOA_g and WAg (with 4.2 at.% Ag [15]) films measured by EDX and XPS)

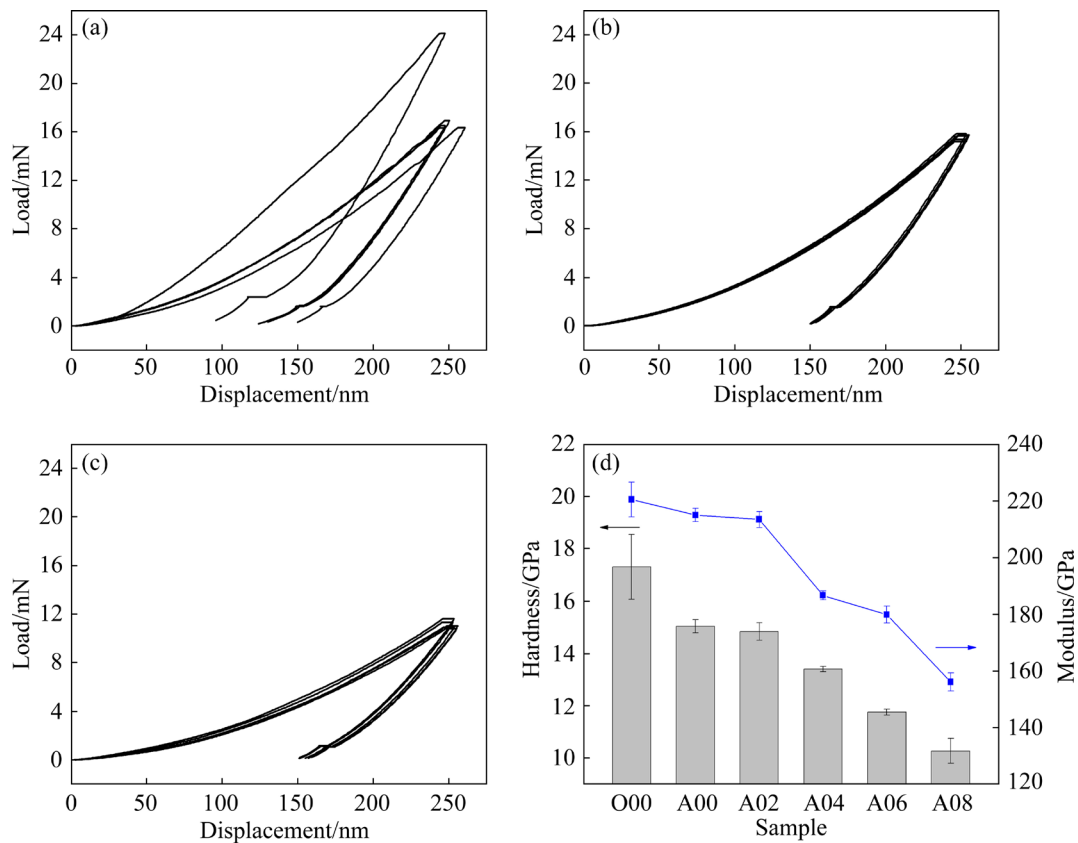


Fig. 6 Load–displacement curves (a–c) and nanohardness and elastic modulus (d) of film samples with silicon substrate measured with maximum displacement of 250 nm during loading: (a) O00; (b) A00; (c) A08

film is not smooth on the surface and even cracking and peeling off will occur. The rough surface has varied the indentation curves. Hardness of the pure W film is as high as 17.3 GPa, and the addition of oxygen decreases the hardness to 15.0 GPa (Fig. 6(d)). With the further addition of silver, the hardness is gradually decreased to 10.3 GPa for Sample A08. The films are still much harder than the pure silver film (HV 240 [20]). The elastic modulus also shows the decreasing trend with the

addition of oxygen and silver. The high hardness and modulus would be good for wear resistance of the WOA_g coatings.

Corrosion behavior of the steel samples was assessed by potentiodynamic polarization test (Fig. 7). The coated samples have lower corrosion potential (ϕ_o), larger corrosion current density (J_o) and passive current density (J_p) values than the polished sample (Table 2), indicating the lower anticorrosion property of the W-based films. The

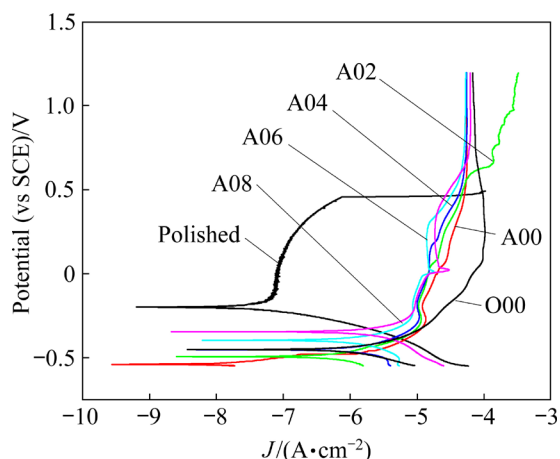


Fig. 7 Potentiodynamic polarization plots of polished, W, WO and WOAg coated stainless steel samples

Table 2 Corrosion data of polished and coated stainless steel samples

Sample	$J_o/(\mu\text{A}\cdot\text{cm}^{-2})$	$\phi_o(\text{vs SCE})/\text{V}$	$J_p/(\mu\text{A}\cdot\text{cm}^{-2})^*$
Polished	0.05	-0.20	0.08
O00	1.94	-0.45	96.52
A00	0.40	-0.54	29.62
A02	1.45	-0.49	21.84
A04	7.55	-0.45	15.80
A06	6.71	-0.40	14.12
A08	9.28	-0.35	18.99

* at 0.14 V vs SCE

WOAg film samples show similar polarization plots, and the ϕ_o value shifts in the noble direction with the addition of silver. Specially, the current peaks at 3, 16 and 22 mV are observed for Samples A04, A06 and A08, respectively. The current peaks at around 0.08 V were found for the silver-containing ceramic coatings (DLC–Ag [16], TiO₂–Ag [28], MgO–Ag [29], etc) due to the dissolution of silver nanoparticles. The present current peaks evidence nanocomposite structure of the WOAg films, which was observed by SEM.

3.3 Immersion and antibacterial tests analysis

Samples A06 and WAg_{4.2} were soaked in 10 mL pure water for up to 3 d, and the accumulated ion concentrations were measured by ICP-MS (Table 3). Sample A06 (W_{31.1}O_{59.5}Ag_{9.4}) released less silver ions and more tungsten ions than sample WAg_{4.2}, although the former has higher silver content. This can be explained by the

formation of tungsten oxide (Fig. 4) and the depletion of silver (Fig. 5) on the film surface.

Table 3 Accumulated silver and tungsten ion concentrations for Samples WAg_{4.2} and A06 (W_{31.1}O_{59.5}Ag_{9.4}) measured by ICP-MS

Time/ d	Ag concentration/ 10^{-9}		W concentration/ 10^{-6}	
	WAg _{4.2}	A06	WAg _{4.2}	A06
0.5	4.74	3.24	4.13	12.20
1	26.54	4.97	9.07	21.53
3	38.34	8.40	26.47	29.54

The bactericidal activity of the film samples was assessed against *E.coli* by agar plate counting method. Sample A00 and the glass control show many colonies, but for the Ag-containing film samples, the quantity of colonies is gradually decreased with the increase of silver content. The antibacterial ratios are 70%, 71%, 86% and 83% for Samples A02–A08, respectively by taking glass sample as the reference (Fig. 8). If the ions releasing rates are similar in water and in the bacterial suspension, the Ag and W concentrations are calculated to be 0.52 and 1955 $\mu\text{g}/\text{mL}$, respectively for Sample A06. The value of 0.52 $\mu\text{g}/\text{mL}$ is comparable with the reported minimum silver concentration to kill *E.coli* for Ag-doped CaP nanoparticles (0.62 $\mu\text{g}/\text{mL}$ [30]), and is lower than the silver concentration limit for a powerful fungicide (5.4×10^{-6} [31]). Apart from silver, tungsten element also contributes to the antibacterial activity of WOAg and WAg [20] films. The mechanical and biological merits of WOAg films would benefit their potential antimicrobial applications in environmental and other fields.

4 Conclusions

(1) The sputter deposited tungsten film added with oxygen (~60 at.%) has better adhesion and surface smoothness. Oxygen and silver (up to 14.3 at.%) exist mainly as solid solution atoms in the WOAg films, and silver nanoparticles are also observed on the film surface.

(2) The incorporation of silver decreases hardness and changes corrosion behavior of the films. The addition of oxygen has suppressed the release of silver ions from the film in water. The films show good antibacterial activity to *E. coli*.

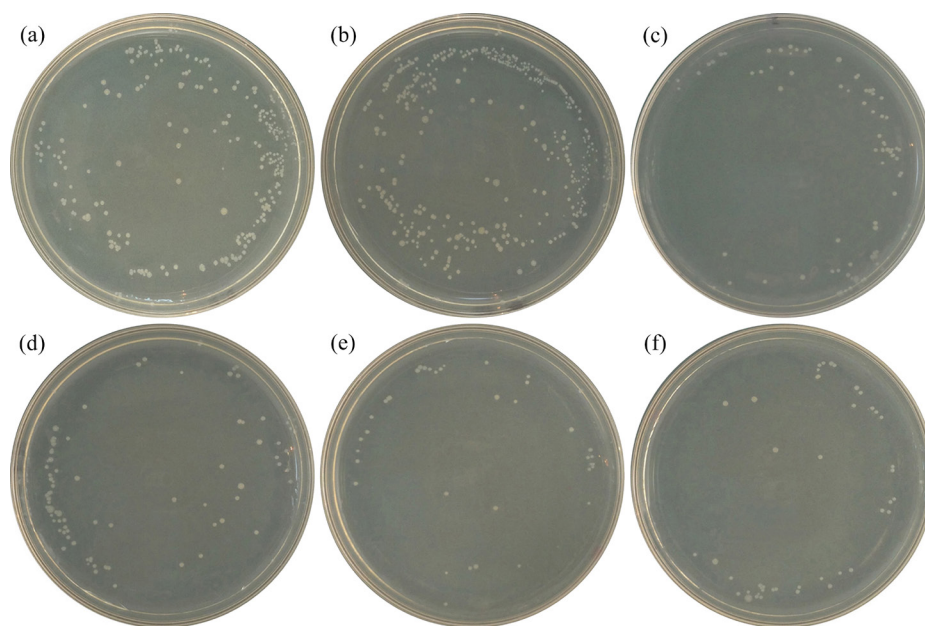


Fig. 8 Representative antibacterial test results of WOAg film samples with glass substrate against *E. coli* by plate counting method: (a) Glass control; (b) A00; (c) A02; (d) A04; (e) A06; (f) A08

(3) These features would be beneficial for potential antimicrobial applications of the WOAg films in environmental and other antimicrobial fields.

Acknowledgments

The authors are grateful for the financial support from the Natural Science Foundation of Shaanxi Province, China (No. 2021JM-036), and would thank the Instrumental Analysis Center of Xi'an Jiaotong University for the assistance in XPS and ICP-MS analyses.

References

- [1] NGUYEN V Q, ISHIHARA M, KINODA J, HATTORI H, NAKAMURA S, ONO T, MIYAHIRA Y, MATSUI T. Development of antimicrobial biomaterials produced from chitin-nanofiber sheet/silver nanoparticle composites [J]. *Journal of Nanobiotechnology*, 2014, 12: 49.
- [2] WANG L J, WANG Y J, SHUM P W, HOU Y F, FU T. Sputter deposited Cr–Ag films for environmental antimicrobial applications [J]. *Coatings*, 2021, 11: 1153.
- [3] CHANG T, SEPATI M, HERTING G, LEYGRAF C, RAJARAO G K, BUTINA K, RICHTER-DAHLFORS A, BLOMBERG E, ODNEVALL WALLINDER I. A novel methodology to study antimicrobial properties of high-touch surfaces used for indoor hygiene applications—A study on Cu metal [J]. *Plos One*, 2021, 16(2): e0247081.
- [4] FONTES D, REYES J, AHMED K, KINZEL M. A study of fluid dynamics and human physiology factors driving droplet dispersion from a human sneeze [J]. *Physics of Fluids*, 2020, 32(11): 111904.
- [5] REDFERN J, TUCKER J, SIMMONS L M, ASKEW P, STEPHAN I, VERRAN J. Environmental and experimental factors affecting efficacy testing of nonporous plastic antimicrobial surfaces [J]. *Methods and protocols*, 2018, 1(4): 36.
- [6] BAKHSHESHI-RAD H R, DAYAGHI E, ISMAIL A F, AZIZ M, AKHAVAN-FARID A, CHEN X. Synthesis and in-vitro characterization of biodegradable porous magnesium-based scaffolds containing silver for bone tissue engineering [J]. *Transactions of Nonferrous Metals Society of China*, 2019, 29(5): 984–996.
- [7] IQBAL N, IQBAL S, IQBAL T, BAKHSHESHI-RAD H R, ALSAKKAF A, KAMIL A, ABDUL KADIR M R, IDRIS M H, RAGHAV H B. Zinc-doped hydroxyapatite-zeolite/polycaprolactone composites coating on magnesium substrate for enhancing in-vitro corrosion and antibacterial performance [J]. *Transactions of Nonferrous Metals Society of China*, 2020, 30(1): 123–133.
- [8] ZHENG L, QIAN S, LIU X Y. Induced antibacterial capability of TiO₂ coatings in visible light via nitrogen ion implantation [J]. *Transactions of Nonferrous Metals Society of China*, 2020, 30(1): 171–180.
- [9] KAWAKAMI H, YOSHIDA K, NISHIDA Y, KIKUCHI Y, SATO Y. Antibacterial properties of metallic elements for alloying evaluated with application of JIS Z 2801: 2000 [J]. *Isij International*, 2008, 48(9): 1299–1304.
- [10] CAZALINI E M, MIYAKAWA W, TEODORO G R, SOBRINHO A S S, MATIELI J E, MASSI M, KOGA-ITO C Y. Antimicrobial and anti-biofilm properties of polypropylene meshes coated with metal-containing DLC thin films [J]. *Journal of Materials Science: Materials in Medicine*, 2017, 28(6): 97.
- [11] BELLANTONE M, WILLIAMS H D, HENCH L L. Broad-spectrum bactericidal activity of Ag₂O-doped bioactive glass [J]. *Antimicrobial Agents and Chemotherapy*, 2002, 46(6): 1940–1945.
- [12] REBELO R, CALDERON S V, FANGUEIRO R, HENRIQUES M, CARVALHO S. Influence of oxygen content on the antibacterial effect of Ag–O coatings deposited

- by magnetron sputtering [J]. *Surface & Coatings Technology*, 2016, 305: 1–10.
- [13] LIU Q, LI Y X, QIU J, CHEN M, WANG J, HU J. Antibacterial property and bioadaptability of Ti6Al4V alloy with a silvered gradient nanostructured surface layer [J]. *Rare Metals*, 2022, 41(2): 621–629.
- [14] YU J G, SUN X H, GONG H H, DONG L, ZHAO M L, WAN R X, GU H Q, LI D J. Influence of Ag concentration on microstructure, mechanical properties and cytocompatibility of nanoscale Ti–Ag–N/Ag multilayers [J]. *Surface & Coatings Technology*, 2017, 312: 128–133.
- [15] HSIEH J H, TSENG C C, CHANG Y K, CHANG S Y, WU W. Antibacterial behavior of TaN–Ag nanocomposite thin films with and without annealing [J]. *Surface & Coatings Technology*, 2008, 202(22/23): 5586–5589.
- [16] WANG L J, ZHANG F, FONG A, LAI K M, SHUM P W, ZHOU Z F, GAO Z F, FU T. Effects of silver segregation on sputter deposited antibacterial silver-containing diamond-like carbon films [J]. *Thin Solid Films*, 2018, 650: 58–64.
- [17] CALDERON VELASCO S, CAVALEIRO A, CARVALHO S. Functional properties of ceramic–Ag nanocomposite coatings produced by magnetron sputtering [J]. *Progress in Materials Science*, 2016, 84: 158–191.
- [18] WOJCIESZAK D, MAZUR M, KACZMAREK D, MAZUR P, SZPONAR B, DOMARADZKI J, KEPINSKI L. Influence of the surface properties on bactericidal and fungicidal activity of magnetron sputtered Ti–Ag and Nb–Ag thin films [J]. *Materials Science & Engineering C*, 2016, 62: 86–95.
- [19] BAI L, HANG R, GAO A, ZHANG X, HUANG X, WANG Y, TANG B, ZHAO L, CHU P K. Nanostructured titanium–silver coatings with good antibacterial activity and cytocompatibility fabricated by one-step magnetron sputtering [J]. *Applied Surface Science*, 2015, 355: 32–44.
- [20] WANG L J, ZHANG F, FONG A, LAI K M, SHUM P W, ZHOU Z F, FU T, NING P, YANG S Y. Tungsten film as a hard and compatible carrier for antibacterial agent of silver [J]. *Journal of Materials Science*, 2018, 53(15): 10640–10652.
- [21] PEUSTER M, FINK C, WOHLSEIN P, BRUEGMANN M, GÜNTHER A, KAESE V, NIEMEYER M, HAFERKAMP H, VON SCHNAKENBURG C V. Degradation of tungsten coils implanted into the subclavian artery of New Zealand white rabbits is not associated with local or systemic toxicity [J]. *Biomaterials*, 2003, 24(3): 393–399.
- [22] CHENG J, LIU B, WU Y H, ZHENG Y F. Comparative in vitro study on pure metals (Fe, Mn, Mg, Zn and W) as biodegradable metals [J]. *Journal of Materials Science & Technology*, 2013, 29(7): 619–627.
- [23] POLCAR T, CAVALEIRO A. Structure, mechanical properties and tribology of W–N and W–O coatings [J]. *International Journal of Refractory Metals & Hard Materials*, 2010, 28(1): 15–22.
- [24] ADESINA A Y, DRMOSH Q A, KUMAR A M, MOHAMEDKHAIR A K. Post-annealing effect on the electrochemical behavior of nanostructured magnetron sputtered W₃O films in chloride- and acid-containing environments [J]. *Surface & Coatings Technology*, 2021, 420: 127334.
- [25] HUANG Hui-min, CHEN Xin-min. Metastable characteristics of β -W [J]. *Acta Metallurgica Sinica*, 1988, 24(6): 494–498.
- [26] WEN S P, GUO J G. Development of arrayed nanoporous Ag/W films by alternate deposition [J]. *Materials Technology*, 2013, 28(3): 165–168.
- [27] PENG M J, YANG J J, ZHANG F F, LU C Y, WANG L M, LIAO J L, YANG Y Y, LIU N. Improved irradiation tolerance of W thin films with homogeneously multilayered structure [J]. *Surface & Coatings Technology*, 2017, 313: 230–235.
- [28] FU T, SHEN Y G, ALAJMI Z, YANG S Y, SUN J M, ZHANG H M. Sol-gel preparation and properties of Ag–TiO₂ films on surface roughened Ti–6Al–4V alloy [J]. *Materials Science and Technology*, 2015, 31(4): 501–505.
- [29] ALAJMI Z, FU T, ZHAO Y J, YANG S Y, SUN J M. Ag-enhanced antibacterial property of MgO film [J]. *Materials Science Forum*, 2016, 859: 90–95.
- [30] PEETSCH A, GREULICH C, BRAUN D, STROETGES C, REHAGE H, SIEBERS B, KÖELLER M, EPPLE M. Silver-doped calcium phosphate nanoparticles: Synthesis, characterization, and toxic effects toward mammalian and prokaryotic cells [J]. *Colloids and Surfaces B*, 2013, 102: 724–729.
- [31] HEIDENAU F, MITTELMEIER W, DETSCH R, HAENLE M, STENZEL F, ZIEGLER G, GOLLWITZER H. A novel antibacterial titania coating: Metal ion toxicity and in vitro surface colonization [J]. *Journal of Materials Science: Materials in Medicine*, 2005, 16(10): 883–888.

用于环境抗菌的氧稳定 W–Ag 薄膜

付涛¹, 王丽君¹, 王应杰¹, 陈东圳², 沈步云³

1. 西安交通大学 生命科学与技术学院 生物医学信息工程教育部重点实验室, 西安 710049;

2. 西安工程大学 材料科学与工程学院, 西安 710048;

3. 朝日集团有限公司, 香港 观塘

摘要: 在溅射沉积的钨薄膜中加入氧以降低薄膜的残余应力, 进一步添加含量高达 14.3%(摩尔分数)的银以进行抗菌功能化。采用 SEM-EDX、XPS 和 XRD 分析薄膜。薄膜仅检测到 β -W 或 W₃O 相的 X 射线衍射峰。氧和银主要以固溶原子的形式存在于薄膜中。银的加入降低了薄膜的硬度(仍然 ≥ 10.3 GPa)和弹性模量。动电位极化实验表明 WO 膜的腐蚀电流密度低于钨膜, 而银改变了膜层的腐蚀行为。薄膜表面的贫银氧化钨层抑制了银离子在水中的释放, WOAg 膜对大肠杆菌具有良好的抗菌活性。WOAg 薄膜将在环境和其他抗菌应用中发挥作用。

关键词: 钨薄膜; 氧化钨; 银析出; 残余应力; 抗菌涂层